NeuroImage: Clinical 24 (2019) 102088

Contents lists available at ScienceDirect

NeuroImage: Clinical

journal homepage: www.elsevier.com/locate/ynicl

Disrupted functional and structural connectivity within default mode network contribute to WMH-related cognitive impairment

Chen Xin[a,1], Huang Lili[a,1], Ye Qing[a], Yang Dan[a], Qin Ruomeng[a], Luo Caimei[a], Li Mengchun[a], Zhang Bing[d], Xu Yun[a,b,c,*]

[a] Department of Neurology, Affiliated Drum Tower Hospital, Jiangsu Key Laboratory for Molecular Medicine, Nanjing University Medical School, Nanjing, 210008, China
[b] Jiangsu Province Stroke Center for Diagnosis and Therapy, Nanjing, 210008, China
[c] Nanjing Neuropsychiatry Clinic Medical Center, Nanjing, 210008, China
[d] Department of Radiology, Affiliated Drum Tower Hospital, Nanjing University Medical School, Nanjing, 210008, China

ARTICLE INFO

Keywords:
White matter hyperintensities
Cognitive impairment
Default mode network
Functional connectivity
Structural connectivity

ABSTRACT

Aims: The prevalence of white matter hyperintensities (WMH) rises dramatically with aging. Both the progression of WMH and changing patterns of default mode network (DMN) have been proven to be closely associated with cognitive function. The present study hypothesized that changes in functional connectivity and structural connectivity of DMN contributed to WMH related cognitive impairment.

Methods: A total of 116 subjects were enrolled from the Cerebral Small Vessel Disease Register in Drum Tower Hospital of Nanjing University, and were distributed across three categories according to Fazekas rating scale: WMH I (n = 57), WMH II (n = 34), and WMH III(n = 25). All participants underwent neuropsychological tests and multimodal MRI scans, including diffusion tensor imaging and resting-state fMRI imaging. The alterations of functional connectivity and structural connectivity within the DMN were further explored.

Results: Age and hypertension were risk factors for WMH progression. Subjects with a higher WMH burden displayed higher DMN functional connectivity in the medial frontal gyrus, while lower DMN functional connectivity in the thalamus. After adjusting for aging, gender, and education, the increased DMN functional connectivity in the medial frontal gyrus, and the increased mean diffusivity of the white matter tracts between the hippocampus and posterior cingulate cortex were independent indicators of worse performance in memory. Moreover, the decreased DMN functional connectivity in the thalamus and increased mean diffusivity of the white matter tracts between the thalamus and posterior cingulate cortex were independent risk factors for a slower processing speed.

Conclusion: The changes in functional connectivity and structural connectivity within the DMN attributed to WMH progression were responsible for the development of cognitive impairment.

ANG:	angular gyrus;
ACC:	anterior cingulate cortex;
CI:	confidence interval;
DMN:	default mode network;
DTI:	diffusion tensor imaging;
FLAIR:	fluid-attenuated inversion recovery;
FA:	fractional anisotropy;
FC:	functional connectivity;
IPC:	inferior parietal cortex;
LTC:	lateral temporal cortex;
MD:	mean diffusivity;
MFG:	medial frontal gyrus;
MTC:	medial temporal cortex;
MMSE:	Mini Mental State Examination;
MoCA:	Montreal Cognitive Assessment;
OR:	odds ratio;
PCC:	posterior cingulate cortex;
ROIs:	regions of interest;
rs-fMRI:	resting-state functional MRI;
SC:	structural connectivity;
SFC:	superior frontal cortex;
WMH:	white matter hyperintensities.

* Corresponding author at: Department of Neurology, Affiliated Drum Tower Hospital, Jiangsu Key Laboratory for Molecular Medicine, Nanjing University Medical School, Nanjing, 210008, China
E-mail address: xuyun20042001@aliyun.com (Y. Xu).
[1] These authors have contributed equally to this work.

https://doi.org/10.1016/j.nicl.2019.102088
Received 8 August 2019; Received in revised form 7 November 2019; Accepted 9 November 2019
Available online 12 November 2019

1. Introduction

White matter hyperintensities (WMH) is described as hyperintense in the subcortical white matter displayed on T2-weighted MRI images and fluid-attenuated inversion recovery (FLAIR) images (Pantoni, 2010). WMH is a state of chronic hypoperfusion in the white matter, which results in demyelination as a consequence of repeated selective oligodendrocyte death (Petito et al., 1998; Promjunyakul et al., 2015; Shi et al., 2016; van Dalen et al., 2016). The proportion of WMH in the general population aged 60 to 90 years is nearly 90% in the European population (Alber et al., 2019), and the prevalence of WMH is as high as 70% in the Chinese population (Han et al., 2018).

WMH has been reported to correlate closely with cognitive impairment, especially in domains of executive function, attention, and processing speed (Debette and Markus, 2010). Many studies have addressed the association between WMH and cognitive impairment (Wong et al., 2019; Zhang et al., 2019), but an important issue arises, i.e., how to predict which individuals with WMH would develop cognitive impairment. The Framingham Offspring Study revealed that WMH volume, no matter whether mild or extensive, was related to an increased risk of cognitive impairment at an age of 60 years or older (Debette et al., 2010). The PROGRESS study demonstrated that severe WMH load, rather than mild or moderate WMH, was an independent predictor of dementia and cognitive decline (Dufouil et al., 2009). It should be noted that WMH has been detected in nearly 80% of the healthy elderly between 60 and 82 years old (Lampe et al., 2019) while a portion of these do not develop cognitive impairment. The relationship between WMH burden and cognitive impairment may be not linear and direct, and the potential mechanisms remain unclear.

Resting-state functional MRI (rs-fMRI) is a non-invasive imaging technique used to explore the aberrant intrinsic functional architecture of the brain, and rs-fMRI provides us with a promising viewpoint to explore spontaneous neural activity in patients with WMH. Using rs-fMRI technology, a series of resting-state networks have been identified based on the temporal correlations among intrinsic fluctuations of blood-oxygen-level-dependent signals across functionally related areas, also known as functional connectivity (FC) (Damoiseaux et al., 2006). Among the networks, default mode network (DMN), has received increasing attention in studies on neuropsychological diseases. DMN is thought to be related to internally directed cognitions (Buckner et al., 2008). Recent studies have found that disrupted DMN patterns had a considerable impact on cognitive dysfunction in Alzheimer's disease (Hodgetts et al., 2018), Parkinson's disease (Diez-Cirarda et al., 2018), and other neurological disorders (Mohan et al., 2016). Our recent studies found both decreased and increased FC of the DMN in subjects with WMH, but havenot shown the association between the altered FC of the DMN and cognitive impairment (Liu et al., 2019a, 2019b). WMH burden can be diveded into 3 grades according to Fazekas grade, and the relationship between the DMN and cognition in WMH subjects may vary depending on the burden level of the WMH. Exploring this relationship with the progression of WMH burden may contribute to the understanding of mechanisms underlying the relationship betweenWMH, DMN, and cognitive impairment. However, the impact of different grades of WMH has not been considered by previous studies.

The DMN mainly comprises the posterior cingulate cortex (PCC), the anterior cingulate cortex (ACC), lateral temporal cortex (LTC), medial temporal cortex (MTC), the medial frontal gyrus (MFG), the inferior parietal cortex (IPC), the angular gyrus (ANG), and the subcortical regions such as the thalamus (Greicius et al., 2003). Actually, these regions are also interconnected via white matter tracts in the structure. The PCC, a core area of the network, is known to have monosynaptic connections with MTC and is structurally connected with the MFG via the cingulum bundle. The PCC is also connected with the IPC via the angular/lateral parietal lobule white matter tracts and the precuneus/posterior cingulate white matter tracts (Greicius et al., 2009; Khalsa et al., 2014). In other words, the core of the DMN is also the structural core connecting other structural modules in structural networks (Hagmann et al., 2008). While FC strength is defined using fMRI data, structural connectivity (SC) strength can be measured with diffusion tensor imaging (DTI) parameters, such as the mean diffusivity (MD) and fractional anisotropy (FA), both of which describe the microstructural integrity of the white matter tracts.

The present study hypothesized that cognitive impairment in elderly subjects with WMH would be related not only to the DMN FC, but also to the altered integrity of the white matter tracts connecting functional modules in the DMN. Therefore, we aimed to investigate the DMN patterns and the related integrity of the white matter tracts in subjects with different grades of WMH, and to explore the relationship between cognitive impairment, the DMN FC, the DMN SC, and the WMH burden.

2. Materials and methods

2.1. Participants

This research was a part of the Study on Register and the Diagnosis, Therapy and Prognosis of Cerebral Small Vessel Disease, an ongoing longitudinal study of cerebral small vessel disease conducted in the Affiliated Drum Tower Hospital of Nanjing University (Registration number : ChiCTR-OOC-17,010,562). All of the subjects in this study were consecutively recruited from December 2016 to September 2018, the inclusion criteria included: 1) age $\geq$ 50, 2) without MRI contraindications, 3) education level $\geq$ 3 years and could cooperate with neuropsychological assessments, 4) with mild to severe WMH, 5) no recent small subcortical infarction, 6) the number of lacunes $\leq$ 5, and 7) no cerebral microbleeds. The exclusion criteria were as follows: 1) parenchymal hemorrhage or subarachnoid hemorrhage; 2) history of ischemic stroke (diameter of infarct $>$ 15 mm) or cardiogenic cerebral infarction; 3) large vessel diseases, such as vertebral artery or carotid artery stenosis($>$75%); 4)other neurological diseases (e.g., Parkinson's disease, epilepsy, Alzheimer's disease, multiple sclerosis, and neuromyelitis optica); 5) systemic disease(cancer, shock, systemic lupus erythematosus, or thyroid dysfunction); 6) psychiatric disease; and 7) severe decline of vision or audition. A total of 116 subjects were enrolled. To explore brain network patterns related to varying burden of WMH, the subjects were divided into 3 groups according to the Fazekas rating scale (Hasan et al., 2019; Wahlund et al., 2001): WMH I (n = 57), WMH II (n = 34), and WMH III (n = 25). All of the subjects completed a standardized study questionnaire including age, gender, years of education, and the presence of cardiovascular risk factors including hypertension, diabetes mellitus, smoking, and drinking history.

All participants were right-handed and provided written informed consent in accordance with the Declaration of Helsinki. The protocol was approved by the Medical Ethics Committee at our hospital.

2.2. Imaging analysis

2.2.1. Magnetic resonance imaging acquisition

Magnetic resonance images were acquired using a 3.0-Tesla MR scanner (Ingenia 3.0T, Philips Medical Systems, Eindhoven, Netherlands) with a 32-channel head coil. Tight but comfortable foam padding was used to minimize head motion, additionally a pair of earplugs was used to lessen scanner noise. Resting-state functional images, including 230 vol, were acquired by a gradient- echo-planar imaging (GRE-EPI) sequence: repetition time = 2000 ms, echo time = 30 ms, flip angle = 90°, matrix = 64 × 64, voxel size = 3 × 3 × 3 mm, field of view = 192 × 192 mm, thickness = 4.0 mm, gap = 0 mm, and number of slices = 35. The total scan duration was 8 min and 7 s and participants were instructed to keep their eyes closed and stay as still as possible, not to fall asleep or think of anything in particular. The imaging parameters of DTI were as follows: repetition time = 17,379 ms, echo time = 55 ms, flip

angle = 90°, matrix = 112 × 110, voxel size = 2 × 2 × 2.5 mm, thickness = 2.5 mm, and number of slices = 55. There were 32 diffusion-weighted volume directions and one non-diffusion weighted volume. The diffusion weighting was equal to a b-value of 1000s/mm^2. Total scan duration was 11min and 15 s. Three-dimensional (3D) T1-weighted turbo fast echo sagittal images with high resolution were acquired with the following parameters: repetition time = 9.8 ms, echo time = 4.6 ms, flip angle = 8°, matrix = 256 × 256, field of view = 256 × 256 mm, voxel size = 1 × 1 × 1 mm, thickness = 1.0 mm, gap = 0 mm, and number of slices = 192. 3D FLAIR sagittal images were obtained with the following imaging parameters: repetition time = 4500 ms, echo time = 344 ms, flip angle = 90°, matrix = 272 × 272, thickness = 1.0 mm, gap = 0 mm, and number of slices = 200. Besides, each subject underwent routine axial T2-weighted sequences and diffusion weighted imaging.

2.2.2. Image preprocessing

Rs-fMRI preprocessing was performed using the Data Processing and Analysis of Brain Imaging (DPABI 2.3, http://rfmri.org/DPABI) software (Yan et al., 2016), which is based on statistical parametric mapping (SPM12, http://www.fil.ion.ucl.ac.uk/spm). The first ten vol from each subject were discarded to account for the signal equilibrium and the subjects' adaptation to the scanning noise. The remaining 220 vol were corrected for acquisition-time differences between the slices and were subsequently realigned to the first volume. Afterwards, the head motion parameters were calculated, and no participants head motion exceeded 3 mm in x, y, or z translation or 3° in rotation. The resulting functional data were spatially normalized to the Montreal Neurological Institute (MNI) space (using the mean EPI image as the source volume), resampled into 3 × 3 × 3 mm voxels and smoothed with a Gaussian kernel of 6 × 6 × 6 mm. Removal of confounding signals, such as Friston-24 head motion parameters, white matter, cerebrospinal fluid, and whole brain, from the smoothed functional images were performed via regression analysis following these procedures.

The DICOM images of DTI were firstly loaded into FSL (https://fsl.fmrib.ox.ac.uk/fsl/fslwiki/), the images were corrected for eddy current distortion and head motion, and then the b matrix was reoriented accordingly. The tensor model was fitted using a nonlinear least square fitting procedure. Finally, the scalar maps including FA and MD were calculated and exported using Diffusion Toolkit (www.trackvis.org, version 0.6.4.1). The whole brain tractography was performed with an FA threshold of 0.2 and an angle threshold of 45° and was afterwards imported into TrackVis (www.trackvis.org, version 0.6.1) for virtual dissections.

2.2.3. FC analysis

Seed-based FC analysis was used to construct the resting-state DMN. We selected 6 mm radius spheres centered at the PCC (MNI space: −2, −45, 34), which served as the seed region for the DMN. For each subject, a mean time series of PCC was computed as the reference time course for the DMN. Pearson cross-correlation analysis was applied between the seed time course and the time course of the whole brain voxels, and then the Fisher's z-transformation was used to improve the normality of the correlation coefficients. Ultimately, the FC map of each subject was obtained. To construct the DMN, a one sample *t*-test was used to identify the brain regions that positively correlated with the PCC in all subjects. The threshold was set at a corrected $P < 0.001$, determined by Monte Carlo simulation for multiple comparisons (voxel-wise $P < 0.001$, FWHM = 6 mm, cluster size > 486 mm^3). The binary image of the result served as the mask for subsequent intra-DMN analysis. A one-way ANCOVA was performed on maps of three groups using the Resting-State fMRI Data Analysis Toolkit (REST, http://www.restfmri.net), with age, gender, and years of education as covariates. The result was corrected by Monte Carlo simulation with settings of voxel-wise $P < 0.01$, FWHM = 6 mm, and cluster size > 1215mm^3. Finally, the average FC strength of each significant region was extracted in each group for further analysis.

2.2.4. Tractography and virtual dissections

Regions of interest (ROIs) were selected based on the functional analysis. The PCC was the beginning point and significant regions in the FC analysis were end points. Virtual in vivo dissections of the tracts between the ROIs were performed with TrackVis after the corresponding masks of the ROIs were imported into the software. The mean FA and MD between the ROIs were automatically calculated in all subjects.

2.2.5. Fazekas visual rating scale

Two neurologists independently assessed FLAIR sequences and scored the WMH using the Fazekas scale: 0-absence, 1-focal lesions, 2-beginning confluence of lesions, and 3-large confluent areas or diffuse involvement of the entire region. The intraclass correlation coefficients for inter and intra-observer agreements were > 0.90.

2.2.6. Brain and WMH volumetry

Briefly, the volumes of gray matter, white matter, and central spinal fluid were calculated using a VBM8 toolbox (http://dbm.neuro.uni–jena.de/vbm8) on 3D-T1 images. The WMH volumes were automatically computed with the Wisconsin WMH Segmentation Toolbox (Ithapu et al., 2014) (W2MHS, http://pages.cs.wisc.edu/~vamsi/w2mhs.html) on FLAIR and 3D-T1 images. The standardized WMH volume was the ratio of actual total WMH volume to total intracranial volume in each subject.

2.3. Neuropsychological assessments

The Mini Mental State Examination (MMSE) and the Montreal Cognitive Assessment (MoCA) were conducted by a neuropsychologist in a quiet environment to evaluate global cognitive function. The different domains of cognition were identified according to the following tests: Processing speed (i.e., Trail-Making Test A and Stroop B), executive function (i.e., Trail-Making Test B minus A and Stroop C minus B), episodic memory (i.e., Audio Verbal Learning Test long-term delayed recall and Visual Reproduction delayed recall), language (i.e., Boston Naming Test and Category Verbal Fluency), and visuospatial function (i.e., Visual Reproduction Copy and Clock-Drawing Task). Raw scores for all neuropsychological tests were z-transformed according to the means and standard deviations across all the participants. Thereafter, the z-score of each domain was generated by averaging the z-scores of the relevant tests.

2.4. Statistical analysis

Normality of continuous variables was checked by the Kolmogorov–Smirnov test and WMH volumes were transformed using a logarithm function to normalize the distribution. One-way analysis of variance, chi-squared testing, and nonparametric testing were utilized to compare the differences in demographic and neuroimaging characteristics, medical history, and neuropsychological data among the three groups.

The statistical significance of FC, FA, and MD among the three groups was analyzed with analysis of covariance. The spearman correlation analysis was conducted to evaluate the association between Fazekas scores and WMH volume [lg(ml)]. The partial correlation analysis was conducted to assess the FC and clinical neuropsychological variables in the WMH III group, controlling for variables known to affect cognitive function (age, gender, and years of education). An ordinal multi-categorical regression model was applied to analyze the effect of cardiovascular risk factors on WMH with age as covariate. A multivariate linear regression model was performed to analyze the independent effect of FC and SC on cognitive function.

All statistics were performed with SPSS v21.0, and the significance

Table 1
Demographic and neuroimaging characteristics.

Items	WMH I	WMH II	WMH III	p-value
Age	58.00(11.00)	66.35 ± 7.26[a]	70.24 ± 5.47[a]	<0.001*
Edu	12.00(7.00)	12.00(6.00)	11.24 ± 3.69	0.120
Gender (male:female%)	32:25(56.0:44.0)	19:15(55.9:44.1)	11:14(44.0:56.0)	0.564
Hypertension (yes:no%)	25:32(44.0:56.0)	24:10(70.6:29.4)	22:3(88.0:12.0)	<0.001*
Diabetes (yes:no%)	7:50(12.3:87.7)	8:26(23.5:76.5)	3:22(12.0:88.0)	0.308
Smoking history (yes:no%)	10:47(17.5:82.5)	4:30(11.8:88.2)	3:22(12.0:88.0)	0.688
Drinking history (yes:no%)	9:48(15.8:84.2)	6:28(17.6:82.4)	4:21(16.0:84.0)	0.972
WMH volume(ml)	469.70 ± 214.64	1869.90(772.09)[a]	6614.89(8824.82)[a,b]	<0.001*
lg WMH	2.70(0.33)	3.27 ± 0.13[a]	3.88 ± 0.30[a,b]	<0.001*
lacune	0.00 (1.00)	0.00 (1.00)	1.00 (1.00)	0.062
CMB	0	0	0	/

Note: Values with normal distribution are presented as the mean ± stand deviation (SD); Values with non-normal distribution are presented as median(interquartile). χ^2 test was applied in the comparisons of gender, hypertension, diabetes and smoking history; nonparametric test was applied in the other comparisons. *: $p<0.05$; a: $p<0.05$ differ from WMH I; b: $p<0.05$ differ from WMH II. Abbreviations: WMH, white matter hyperintensity; CMB, cerebral microbleeds.

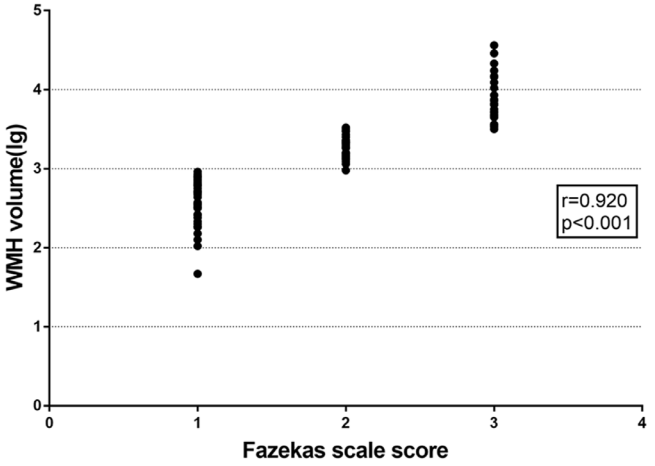

Fig. 1. Scatterplot showing the association of Fazekas scale scores and WMH volume [lg(ml)]. Fazekas scores were significantly correlated with WMH volume ($r = 0.920$, $P<0.001$). Abbreviations: WMH, white matter hyperintensities.

Table 2
Association of cardiovascular risk factors with WMH Fazekas scale scores.

	OR	95% CI	p-value
Hypertension	3.077	1.245–7.606	0.015
Diabetes	1.339	0.466–3.850	0.588
Smoking history	1.168	0.262–5.201	0.838
Drinking history	3.699	0.934–14.64	0.062

Note: An ordinal multi-categorical regression model was applied to analyze the effect of cardiovascular risk factors on WMH with age as covariate. Abbreviations: WMH, white matter hyperintensity; OR, odds ratio; CI indicates confidence interval.

level was set at $P< 0.05$.

3. Results

3.1. Demographics, neuroimaging and neuropsychological data analysis

Table 1 summarizes the participants' demographic and neuroimaging characteristics. Gender, education, history of diabetes, smoking and drinking history, and the number of lacune were comparable among the three groups. Notably, the subjects in the WMH II and WMH III groups were obviously older and more hypertensive than the subjects in the WMH I group. Table 1&Fig. 1 also showed that higher Fazekas scores were highly correlated with a higher WMH volume ($r = 0.920$, $P<0.001$). In the ordinal multi-categorical regression analysis (Table 2), hypertension was an independent predictor of WMH severity, and controlling for age, individuals with hypertension had an odds ratio (OR) of 3.077(95% confidence interval (CI): 1.245–7.606) for one grade higher on the Fazekas scale.

Table 3
Neuropsychological data.

Items	WMH I	WMH II	WMH III	p-value
Globe cognitive function				
MMSE	29.00(2.00)	28.00(2.00)	28.00(2.00)[a]	<0.001*
MoCA	27.00(3.00)	25.00(5.00)[a]	24.00(6.00)[a]	<0.001*
Processing speed				
TMT A(s)	41.00(20.00)	59.58 ± 20.36[a]	65.00(26.00)[a]	<0.001*
Stroop B(s)	19.50(8.00)	21.00(9.00)	25.45 ± 7.69[a]	0.007*
Z score	−0.29 ± 0.65	0.13 ± 0.84[a]	0.48 ± 0.87[a]	<0.001*
Executive function				
TMT B-A(s)	31.00(28.00)	52.00(57.00)[a]	72.50(67.00)[a]	<0.001*
Stroop C-B(s)	11.00(11.00)	11.00(14.00)	15.50 ± 10.22	0.492
Z score	−0.25 ± 0.45	0.16 ± 0.85[a]	0.36 ± 0.87[a]	<0.001*
Episodic memory				
AVLT-LDR	5.38 ± 2.23	5.00(4.00)[a]	3.00(3.00)[a]	0.001*
VR-DR..	10.00(4.00)	7.26 ± 3.46[a]	6.90 ± 4.38[a]	<0.001*
Z score	0.36 ± 0.74	−0.27 ± 0.64[a]	−0.47 ± 0.73[a]	<0.001*
Language				
BNT	54.50(7.00)	53.00(9.00)[a]	49.70 ± 5.94[a]	0.005*
CVF	18.41 ± 4.42	17.00(4.00)	16.65 ± 3.83	0.063
Z score	0.24 ± 0.76	−0.18 ± 0.79[a]	−0.31 ± 0.82[a]	0.004*
Visual spatial function				
VR copy	14.00(0.00)	14.00(0.00)	14.00(0.00)	0.071
CDT	4.00(0.00)	4.00(0.00)	4.00(0.00)	0.731
Z score	0.32(0.00)	0.32(0.48)	0.32(0.00)	0.552

Note: Values with normal distribution are presented as the mean ± stand deviation (SD); Values with non-normal distribution are presented as median (interquartile). One-way ANOVA was applied in the comparisons of Z scores in processing speed, executive function, episodic memory, language; independent nonparametric test was applied in the other comparisons. *: $p<0.05$; a: $p<0.05$ differ from WMH I; b: $p<0.05$ differ from WMH II. Abbreviations: WMH, white matter hyperintensity; MMSE, Mini Mental State Examination; MoCA, Montreal Cognitive Assessment; TMT, Trail-Making Test; AVLT-LDR, Audio Verbal Learning Test long-term delayed recall; VR-DR.., Visual Reproduction delayed recall; BNT, Boston Naming Test; CVF, Category Verbal Fluency; CDT, Clock-Drawing Task.

As shown in Table 3, subjects in the WMH II and WMH III groups displayed lower scores for global cognitive function (MMSE and MoCA) as compared to the WMH I group, they also showed worse performance in each domain of cognitive function (processing speed, executive

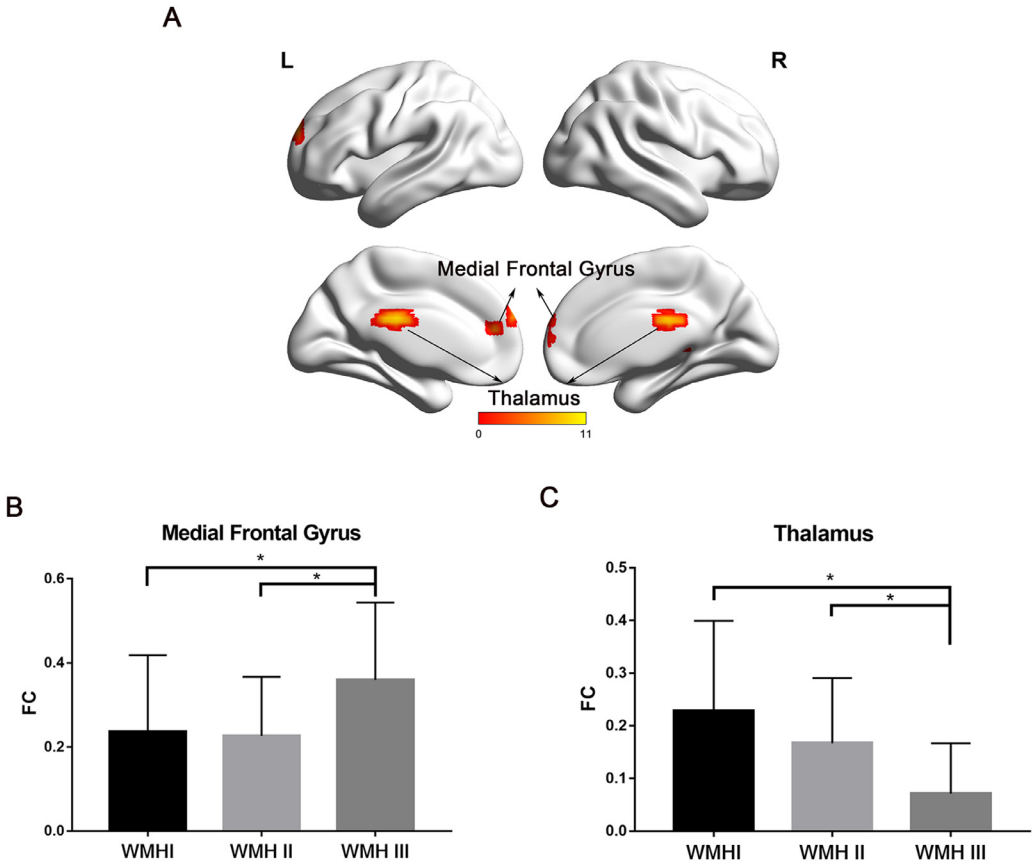

Fig. 2. The group differences of FC. (A) The regions displayed significant difference among the three groups (Thalamus & Medial Frontal Gyrus). The result was corrected by Monte Carlo simulation with settings of voxel-wise $P<0.01$, FWHM = 6 mm, and cluster size > 1215mm^3. The scale was made up of correlation coefficients between PCC and brain regions within DMN and the 11 value in scale expressed the max correlation coefficients. (B) Subjects in the WMH III group displayed significantly greater FC in MFG than the other two groups. (C) Subjects in the WMH III group displayed significantly lower FC in thalamus than the other two groups. * $P<0.05$. Abbreviations: FC, functional connectivity; WMH, white matter hyperintensities; PCC, posterior cingulate cortex; DMN, default mode network; MFG, medial frontal gyrus.

Table 4
Regions showing group differences in FC with PCC.

Brain regions	BA	Peak MNI coordinatesx y z	Peak F value	Number of cluster voxels
Thalamus	Not available	−3 −24 24	10.53	217
Medial Frontal Gyrus	10	3 66 12	9.69	148

Note: BA, Brodmann area; MNI, Montreal Neurological Institute; R, right; $p<0.01$, AlphaSim corrected.

function, episodic memory, and language), and the discrepancy was more apparent in the WMH III group.

3.2. FC analysis

3.2.1. Spatial patterns of DMN

A one-sample *t*-test showed the typical spatial pattern of the DMN in all subjects (voxel-wise $P < 0.001$, FWHM = 6 mm, cluster size > 486 mm3) (Supplementary Figure 1). The PCC-based DMN pattern of the participants included PCC, ACC, ANG, IPC, LTC, MTC, MFG, superior frontal cortex (SFC), and thalamus.

3.2.2. Group differences in DMN

Compared with the WMH I and WMH II groups, patients in the WMH III group displayed prominently increased FC mainly involving the MFG, while there was decreased FC in the thalamus (Fig. 2A). Detailed information about the brain regions is available in Table 4. FC values extracted from the MFG and thalamus showed no significant difference between the WMH I and WMH II groups (Fig. 2B&C).

3.2.3. Correlation analysis

For subjects in the WMH III group, a significant correlation was found between FC strength in the MFG and episodic memory [$r = = -0.467$, $P = 0.029$; 95% CI (−0.796, −0.034) , Fig. 3A]. A strong positive relationship was observed between FC strength in the thalamus and language [$r = 0.502$, $P = 0.017$; 95% CI (0.084, 0.763), Fig. 3B]. Interestingly, the higher the FC strength in the thalamus, the less time spent in processing speed [$r = = -0.528$, $P = 0.012$; 95% CI (−0.800, −0.167), Fig. 3C] and executive function [$r = = -0.504$, $P = 0.017$; 95% CI (−0.802, −0.178), Fig. 3D]. Nonetheless, there was no significant effect of FC in the MFG or thalamus on visual spatial function.

3.3. Microstructural changes of white matter tracts

3.3.1. Selection of ROIs

PCC was the beginning point, meanwhile, the thalamus and MFG were chosen as end points based on the results of FC analysis. Fiber tracts were identified between the PCC and thalamus, while few fiber tracts were detected between the PCC and MFG. Given that the MFG was associated with episodic memory in FC analysis and previous studies of fiber tract connections between the DMN brain regions indicated that there was cingulum hippocampal projection between the PCC and hippocampus[23], thus memory related hippocampal region was selected as another ROI.

3.3.2. Microstructural integrity of fiber tract connection

As shown in Table 5 and Fig. 4A, the mean FA value of the PCC-hippocampus in the WMH III group was the lowest among the groups, even though it did not reach statistical significance. Fig. 4B shows that the mean MD value of the PCC-hippocampus in the WMH III group was apparently higher than the former two groups. A similar trend was also observed in the white matter tracts from the PCC to thalamus (Table 5, Fig. 4C&D).

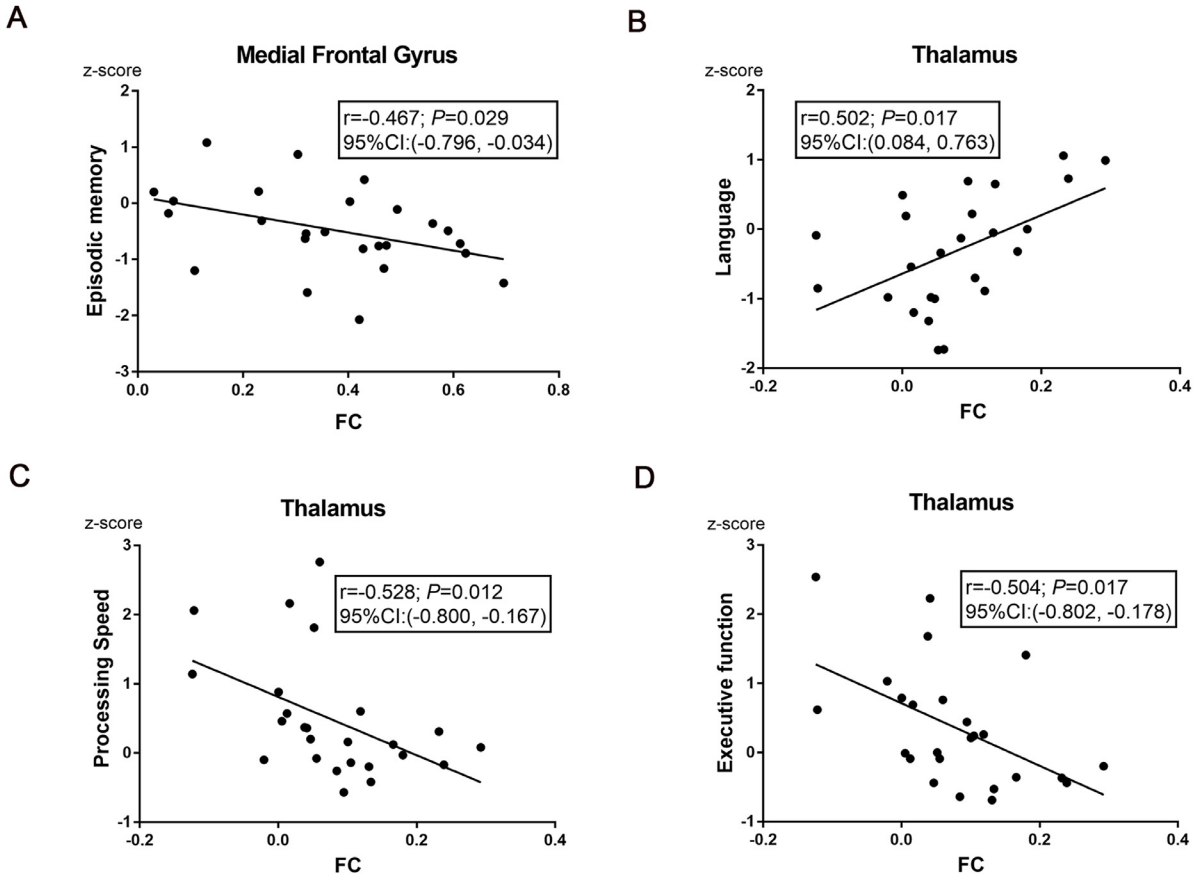

Fig. 3. Correlation analyses between cognitive function and FC in the WMH III group. (A) FC of PCC- MFG was negatively correlated with episodic memory [$r = = -0.467$, $P = 0.029$; 95% CI (-0.796, -0.034)]. (B) FC of PCC-thalamus was positively correlated with language [$r = 0.502$, $P = 0.017$; 95% CI (0.084, 0.763)]. (C) FC of PCC-thalamus was negatively correlated with the time of processing speed [$r = = -0.528$, $P = 0.012$; 95% CI (-0.800, -0.167)]. (D) FC of PCC-thalamus was negatively correlated with the time of executive function [$r = = -0.504$, $P = 0.017$; 95% CI (-0.802, -0.178)]. The scores of each domain were z-transformed scores of the relevant tests. Correlation analyses were performed after adjustment of covariates (sex, age, and years of education). Abbreviations: FC, functional connectivity; WMH, white matter hyperintensities; PCC, posterior cingulate cortex; MFG, medial frontal gyrus; CI, confidence interval.

Table 5
DTI parameters in relation to Fazekas rating scale.

		WMH I	WMH II	WMH III	F	P-value
PCC-—Hippocampus	FA	0.556541 ± 0.045732	0.547029 ± 0.061682	0.536966 ± 0.046522	2.553	0.082
	MD	0.000866 ± 0.000115	0.000855 ± 0.000065	0.000939 ± 0.000124[a,b]	4.094	0.019*
PCC-Thalamus	FA	0.546813 ± 0.033147	0.536131 ± 0.044079	0.521685 ± 0.036568[a]	8.526	<0.001*
	MD	0.000799 ± 0.000072	0.000817 ± 0.000032	0.000869 ± 0.000057[a,b]	5.991	0.003*

Note: Values are presented as the mean ± stand deviation (SD). Analysis of covariance was applied in the comparisons of FA and MD values. *: $p < 0.05$; a: $p < 0.05$ differ from WMH I; b: $p < 0.05$ differ from WMH II. Abbreviations: DTI, diffusion tensor imaging; WMH, white matter hyperintensities; PCC, posterior cingulate cortex; FA, fractional anisotropy; MD, mean diffusivity.

3.3.3. FC and SC as independent predictors for cognitive impairment

After adjusting for confounding variables (age, gender, and years of education), the increased MD value of the PCC-hippocampus ($\beta = = -2575.319$, $P = 0.040$) and increased FC of the PCC-MFG ($\beta = = -2.560$, $P = 0.006$) were respectively independent risk factors for the decline of episodic memory in the WMH III group (Table 6). In addition, the increased MD value of the PCC-thalamus ($\beta = = 6470.015$, $P = 0.030$) and reduced FC of the PCC-thalamus ($\beta = = -4.294$, $P = 0.007$) were associated with slower speeds in independent task processing (Table 7).

4. Discussion

The present study investigated the FC and SC patterns of the DMN in WMH subjects, and the relationship among FC, SC, and cognitive impairment. We demonstrated that the WMH burden could be exacerbated by aging and hypertension, and the accumulation of WMH burden was associated with altered FC and SC strength within the DMN. Notably, at the phase of severe WMH load, the network function was significantly broken down and the aberrant FC and SC between the PCC and thalamus were independent risk factors for slower processing speeds, and the aberrant FC of the PCC-MFG and SC of the PCC-hippocampus were indicative of memory decline.

Consistent with prior studies (Croall et al., 2018; Tully et al., 2017), the baseline characteristics implied that both hypertension and aging were strong predictors of a high WMH burden. Cerebral small vessel disease is known to be age-related and is closely related to vascular risk factors, including hypertension. The pathogenesis of hypertension includes loss of smooth muscle cells, vessel wall thickening, and lumen restriction (Pantoni, 2010). These pathological features result in

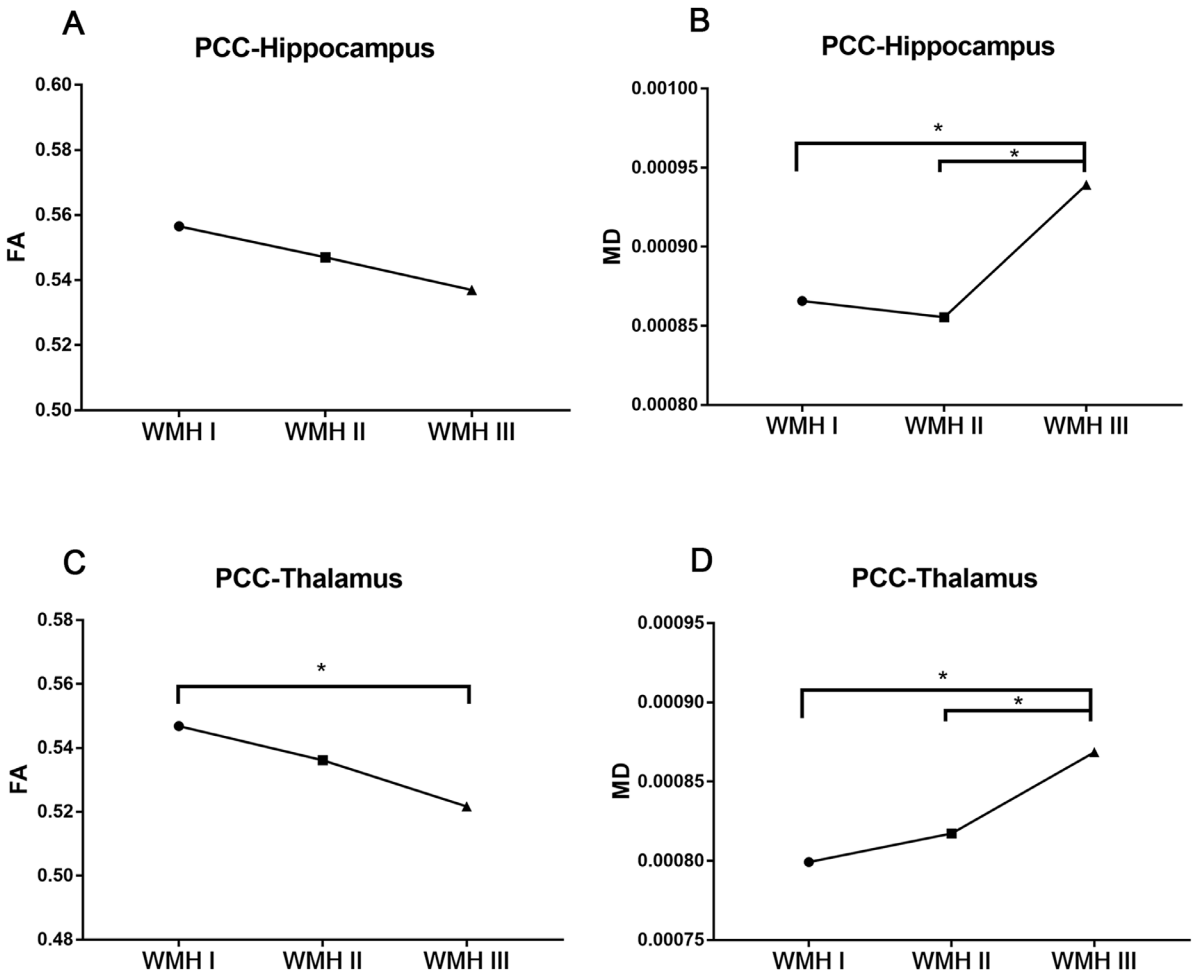

Fig. 4. Comparison of FA or MD values across three groups. (A) The mean FA value of the PCC-hippocampus in the WMH III group was the lowest among the groups, even though it has not reached statistical significance. (B) The mean MD value of the PCC-hippocampus in the WMH III group was significantly higher than the former two groups. (C) The mean FA value of the PCC-thalamus was significantly lower than the former two groups. (D) The mean MD value of the PCC-thalamus was significantly higher than the former two groups. *: $P < 0.05$. Abbreviations: FA, fractional anisotropy; MD, mean diffusivity; PCC, posterior cingulate cortex; WMH, white matter hyperintensities.

Table 6
Multivariate linear regression analysis for Episodic Memory.

	β	P-value
PCC−Hippocampus MD	−2575.319	0.040*
PCC-MFG FC	−2.560	0.006*
Age	0.336	0.236
Sex	−0.026	0.354
Edu	−0.002	0.962

Note: PCC, posterior cingulate cortex; MD, mean diffusivity; MFG, medial frontal gyrus; FC, functional connectivity. *: $p < 0.05$.

Table 7
Multivariate linear regression analysis for Processing Speed.

	β	P-value
PCC-thalamus MD	6470.015	0.030*
PCC-thalamus FC	−4.294	0.007*
Age	0.036	0.204
Sex	−0.166	0.578
Edu	−0.046	0.252

Note: PCC, posterior cingulate cortex; MD, mean diffusivity; FC, functional connectivity. *: $p < 0.05$.

reduced cerebral blood flow, impaired cerebral autoregulation, and subsequent ischemia (Sam et al., 2016). Ischemia, as a consequence of reduced cerebral autoregulation, has been confirmed to result in both demyelination and Wallerian degeneration (Kern et al., 2017), and correlates with the severity of the WMH (Duncombe et al., 2017). Given the important role of hypertension, antihypertensive therapy improving cerebral blood flow is a major area of interest in the treatment of cerebral small vessel disease.

In this study, we found that subjects with a higher WMH burden displayed worse episodic memory, and impaired episodic memory could be related to the increased FC of the PCC-MFG and decreased SC of the PCC-hippocampus. PCC, the core region of the DMN, has the highest metabolic activity during rest and serves as a principal node to cognitive function. Previous studies found that the PCC plays a central role in supporting internally directed cognition and shows increased activity when individuals perform memory retrieval tasks (Buckner et al., 2008; Leech and Sharp, 2014). Patients with amnestic cognitive impairment displayed reduced metabolism in the PCC when compared with healthy subjects (Alexander et al., 2002; Buckner et al., 2005). The MFG encompasses a series of areas that lie along the frontal midline and belongs to the cortical midline subsystem. In the present study, higher FC of the PCC-MFG was related to poorer episodic memory. Increased FC might reflect an impaired balance between synaptic excitation and inhibition, and the loss of the ability to inhibit

activities in the MFG (Bakker et al., 2012; Duverne et al., 2009). This might explain the link between impaired episodic memory and the increased FC of the PCC-MFG. However, several studies found that increased activity or FC in the frontal cortex was associated with better cognitive function in healthy older subjects (Obler et al., 2010; Wierenga et al., 2008) and subjects at risk for dementia (Ye et al., 2017a, 2017b), suggesting that the increased activity or FC might reflect a compensatory recruitment or reallocation of cognitive resources. The compensation may occur in normal aging and the early phase of neurodegenerative diseases. However, as the disease progresses, persistent hyperactivity and hypersynchrony may become harmful for cognitive function. In the present study, the harmful hypersynchrony between PCC and MFG was shown in the WMH III group, which had the heaviest burden of WMH. The hippocampus plays a major role in memory function, and the interaction between the hippocampus and other brain regions involves in the formation, consolidation, and retrieval of episodic memory (Lavenex and Amaral, 2000; Nyberg, 2017; Nyberg et al., 2000). Thus, the decreased SC of the PCC-hippocampus in WMH subjects might have contributed to the impaired episodic memory in the present study. On the other hand, the medial temporal subsystem mainly supports memory retrieval processes. The MTC and MFG appear not to have any direct structural connections, but functional connectivity could exist in the absence of structural connections (Greicius et al., 2009). It is notable that the PCC may mediate and coordinate functional connections between the two regions (Greicius et al., 2009). We found a link between impaired episodic memory and increased FC of the PCC-MFG in subjects of the WMH III group but did not observe a link between impaired episodic memory and the altered FC of the PCC-MTC. Thus, we assume that the increased FC of the PCC-MFG could be more sensitive in detecting the decline of memory than the FC of the PCC-MTC.

The present study also found that the FC and SC of the PCC-thalamus was destroyed with the progression of WMH burden and was related to the decline of processing speed. Previous studies have classified the thalamus as a part of the DMN, and many thalamic nuclei show strong functional connectivity with at least one additional cortical network, such as the dorsal frontoparietal network or sensorimotor network (Hwang et al., 2017). The thalamus is capable of integrating information across multiple functional brain networks according to behavioral context. Accordingly, processing speed reflects ability in the interaction of cognitive processes which are essential for higher order cognitive and mental function. Actually, localized atrophy of the thalamus was related to slower cognitive processing speeds in patients with multiple sclerosis (Bergsland et al., 2016; Bisecco et al., 2018) and Type 2 diabetes mellitus (Chen et al., 2017). Thus, the interaction of the thalamus and other regions play an important role in processing speed. In the present study, damage to the FC and SC between the thalamus and PCC might break down the process of receiving and transmitting signals and as a result, decrease processing speed.

Several limitations should be addressed. First, our study was performed on cross-sectional data. Whether there were causal effects should be explored with longitudinal data. Second, the sample size was relatively small, and our findings should be confirmed with a larger sample. Third, the thalamus can be divided into multiple thalamic nuclei, but we did not perform analyses on each thalamic nucleus. It is not known whether all thalamic nuclei serve as primary hubs to support cognitive functions.

Conclusion

The present study demonstrated that the accumulation of WMH burden was associated with increased FC of the MFG-PCC, decreased FC of the thalamus-PCC, and disrupted SC of the PCC-hippocampus and PCC-thalamus. These aberrant FC and SC were independently associated with slower processing speeds and a poorer memory. Our findings may help to understand the mechanisms underlying the onset of cognitive impairment in WMH subjects, and to explore novel brain markers of vascular cognitive impairment.

Funding

This research was supported by The National Key Research and Development Program of China [2016YFC1300504, 2016YFC0901004], the National Natural Science Foundation of China [81920108017, 81630028], the Key Research and Development Program of Jiangsu Province of China [BE2016610] and Jiangsu Province Key Medical Discipline [ZDXKA2016020]. The funders had no role in the study design, data collection and analysis, decision to publish, or preparation of the manuscript.

Declaration of Competing Interest

The authors declare no conflict of interest with respect to the research, authorship, and/or publication of this article.

Supplementary materials

Supplementary material associated with this article can be found, in the online version, at doi:10.1016/j.nicl.2019.102088.

Reference

Alber, J., Alladi, S., Bae, H.J., Barton, D.A., Beckett, L.A., Bell, J.M., Berman, S.E., Biessels, G.J., Black, S.E., Bos, I., Bowman, G.L., Brai, E., Brickman, A.M., Callahan, B.L., Corriveau, R.A., Fossati, S., Gottesman, R.F., Gustafson, D.R., Hachinski, V., Hayden, K.M., Helman, A.M., Hughes, T.M., Isaacs, J.D., Jefferson, A.L., Johnson, S.C., Kapasi, A., Kern, S., Kwon, J.C., Kukolja, J., Lee, A., Lockhart, S.N., Murray, A., Osborn, K.E., Power, M.C., Price, B.R., Rhodius-Meester, H.F.M., Rondeau, J.A., Rosen, A.C., Rosene, D.L., Schneider, J.A., Scholtzova, H., Shaaban, C.E., Silva, N., Snyder, H.M., Swardfager, W., Troen, A.M., van Veluw, S.J., Vemuri, P., Wallin, A., Wellington, C., Wilcock, D.M., Xie, S.X., Hainsworth, A.H., 2019. White matter hyperintensities in vascular contributions to cognitive impairment and dementia (VCID): knowledge gaps and opportunities. Alzheimers Dement (N Y) 5, 107–117. https://doi.org/10.1016/j.trci.2019.02.001.

Alexander, G.E., Chen, K., Pietrini, P., Rapoport, S.I., Reiman, E.M., 2002. Longitudinal pet evaluation of cerebral metabolic decline in dementia: a potential outcome measure in alzheimer's disease treatment studies. Am. J. Psychiatry 159, 738–745. https://doi.org/10.1176/appi.ajp.159.5.738.

Bakker, A., Krauss, G.L., Albert, M.S., Speck, C.L., Jones, L.R., Stark, C.E., Yassa, M.A., Bassett, S.S., Shelton, A.L., Gallagher, M., 2012. Reduction of hippocampal hyperactivity improves cognition in amnestic mild cognitive impairment. Neuron 74, 467–474. https://doi.org/10.1016/j.neuron.2012.03.023.

Bergsland, N., Zivadinov, R., Dwyer, M.G., Weinstock-Guttman, B., Benedict, R.H., 2016. Localized atrophy of the thalamus and slowed cognitive processing speed in MS patients. Mult. Scler. 22, 1327–1336. https://doi.org/10.1177/1352458515616204.

Bisecco, A., Stamenova, S., Caiazzo, G., d'Ambrosio, A., Sacco, R., Docimo, R., Esposito, S., Cirillo, M., Esposito, F., Bonavita, S., Tedeschi, G., Gallo, A., 2018. Attention and processing speed performance in multiple sclerosis is mostly related to thalamic volume. Brain Imaging Behav. 12, 20–28. https://doi.org/10.1007/s11682-016-9667-6.

Buckner, R.L., Andrews-Hanna, J.R., Schacter, D.L., 2008. The brain's default network: anatomy, function, and relevance to disease. Ann. N. Y. Acad. Sci. 1124, 1–38. https://doi.org/10.1196/annals.1440.011.

Buckner, R.L., Snyder, A.Z., Shannon, B.J., LaRossa, G., Sachs, R., Fotenos, A.F., Sheline, Y.I., Klunk, W.E., Mathis, C.A., Morris, J.C., Mintun, M.A., 2005. Molecular, structural, and functional characterization of Alzheimer's disease: evidence for a relationship between default activity, amyloid, and memory. J. Neurosci. 25, 7709–7717. https://doi.org/10.1523/jneurosci.2177-05.2005.

Chen, J., Zhang, J., Liu, X., Wang, X., Xu, X., Li, H., Cao, B., Yang, Y., Lu, J., Chen, Z., 2017. Abnormal subcortical nuclei shapes in patients with type 2 diabetes mellitus. Eur. Radiol. 27, 4247–4256. https://doi.org/10.1007/s00330-017-4790-3.

Croall, I.D., Tozer, D.J., Moynihan, B., Khan, U., O'Brien, J.T., Morris, R.G., Cambridge, V.C., Barrick, T.R., Blamire, A.M., Ford, G.A., Markus, H.S., 2018. Effect of standard vs intensive blood pressure control on cerebral blood flow in small vessel disease: the preserve randomized clinical trial. JAMA Neurol. https://doi.org/10.1001/jamaneurol.2017.5153.

Damoiseaux, J.S., Rombouts, S.A., Barkhof, F., Scheltens, P., Stam, C.J., Smith, S.M., Beckmann, C.F., 2006. Consistent resting-state networks across healthy subjects. Proc. Natl. Acad. Sci. U S A 103, 13848–13853. https://doi.org/10.1073/pnas.0601417103.

Debette, S., Beiser, A., DeCarli, C., Au, R., Himali, J.J., Kelly-Hayes, M., Romero, J.R., Kase, C.S., Wolf, P.A., Seshadri, S., 2010. Association of mri markers of vascular brain injury with incident stroke, mild cognitive impairment, dementia, and mortality: the framingham offspring study. Stroke 41, 600–606. https://doi.org/10.1161/

strokeaha.109.570044.
Debette, S., Markus, H.S., 2010. The clinical importance of white matter hyperintensities on brain magnetic resonance imaging: systematic review and meta-analysis. BMJ 341, c3666. https://doi.org/10.1136/bmj.c3666.
Diez-Cirarda, M., Strafella, A.P., Kim, J., Pena, J., Ojeda, N., Cabrera-Zubizarreta, A., Ibarretxe-Bilbao, N., 2018. Dynamic functional connectivity in Parkinson's disease patients with mild cognitive impairment and normal cognition. Neuroimage Clin. 17, 847–855. https://doi.org/10.1016/j.nicl.2017.12.013.
Dufouil, C., Godin, O., Chalmers, J., Coskun, O., MacMahon, S., Tzourio-Mazoyer, N., Bousser, M.G., Anderson, C., Mazoyer, B., Tzourio, C., 2009. Severe cerebral white matter hyperintensities predict severe cognitive decline in patients with cerebrovascular disease history. Stroke 40, 2219–2221. https://doi.org/10.1161/strokeaha.108.540633.
Duncombe, J., Kitamura, A., Hase, Y., Ihara, M., Kalaria, R.N., Horsburgh, K., 2017. Chronic cerebral hypoperfusion: a key mechanism leading to vascular cognitive impairment and dementia. Closing the translational gap between rodent models and human vascular cognitive impairment and dementia. Clin. Sci. (Lond) 131, 2451–2468. https://doi.org/10.1042/cs20160727.
Duverne, S., Motamedinia, S., Rugg, M.D., 2009. The relationship between aging, performance, and the neural correlates of successful memory encoding. Cereb. Cortex 19, 733–744. https://doi.org/10.1093/cercor/bhn122.
Greicius, M.D., Krasnow, B., Reiss, A.L., Menon, V., 2003. Functional connectivity in the resting brain: a network analysis of the default mode hypothesis. Proc. Natl. Acad. Sci. U S A 100, 253–258. https://doi.org/10.1073/pnas.0135058100.
Greicius, M.D., Supekar, K., Menon, V., Dougherty, R.F., 2009. Resting-state functional connectivity reflects structural connectivity in the default mode network. Cereb. Cortex 19, 72–78. https://doi.org/10.1093/cercor/bhn059.
Hagmann, P., Cammoun, L., Gigandet, X., Meuli, R., Honey, C.J., Wedeen, V.J., Sporns, O., 2008. Mapping the structural core of human cerebral cortex. PLoS Biol. 6, e159. https://doi.org/10.1371/journal.pbio.0060159.
Han, F., Zhai, F.F., Wang, Q., Zhou, L.X., Ni, J., Yao, M., Li, M.L., Zhang, S.Y., Cui, L.Y., Jin, Z.Y., Zhu, Y.C., 2018. Prevalence and risk factors of cerebral small vessel disease in a Chinese population-based sample. J. Stroke 20, 239–246. https://doi.org/10.5853/jos.2017.02110.
Hasan, T.F., Barrett, K.M., Brott, T.G., Badi, M.K., Lesser, E.R., Hodge, D.O., Meschia, J.F., 2019. Severity of white matter hyperintensities and effects on all-cause mortality in the mayo clinic florida familial cerebrovascular diseases registry. Mayo Clin. Proc. 94, 408–416. https://doi.org/10.1016/j.mayocp.2018.10.024.
Hodgetts, C.J., Shine, J.P., Williams, H., Postans, M., Sims, R., Williams, J., Lawrence, A.D., Graham, K.S., 2018. Increased posterior default mode network activity and structural connectivity in young adult APOE-epsilon4 carriers: a multimodal imaging investigation. Neurobiol. Aging 73, 82–91. https://doi.org/10.1016/j.neurobiolaging.2018.08.026.
Hwang, K., Bertolero, M.A., Liu, W.B., D'Esposito, M., 2017. The human thalamus is an integrative hub for functional brain networks. J. Neurosci. 37, 5594–5607. https://doi.org/10.1523/jneurosci.0067-17.2017.
Ithapu, V., Singh, V., Lindner, C., Austin, B.P., Hinrichs, C., Carlsson, C.M., Bendlin, B.B., Johnson, S.C., 2014. Extracting and summarizing white matter hyperintensities using supervised segmentation methods in Alzheimer's disease risk and aging studies. Hum. Brain Mapp. 35, 4219–4235. https://doi.org/10.1002/hbm.22472.
Kern, K.C., Wright, C.B., Bergfield, K.L., Fitzhugh, M.C., Chen, K., Moeller, J.R., Nabizadeh, N., Elkind, M.S.V., Sacco, R.L., Stern, Y., DeCarli, C.S., Alexander, G.E., 2017. Blood pressure control in aging predicts cerebral atrophy related to small-vessel white matter lesions. Front Aging Neurosci. 9, 132. https://doi.org/10.3389/fnagi.2017.00132.
Khalsa, S., Mayhew, S.D., Chechlacz, M., Bagary, M., Bagshaw, A.P., 2014. The structural and functional connectivity of the posterior cingulate cortex: comparison between deterministic and probabilistic tractography for the investigation of structure-function relationships. Neuroimage 102, 118–127. https://doi.org/10.1016/j.neuroimage.2013.12.022. Pt 1.
Lampe, L., Kharabian-Masouleh, S., Kynast, J., Arelin, K., Steele, C.J., Löffler, M., Witte, A.V., Schroeter, M.L., Villringer, A., Bazin, P.L., 2019. Lesion location matters: the relationships between white matter hyperintensities on cognition in the healthy elderly. J. Cereb. Blood Flow Metab. 39, 36–43. https://doi.org/10.1177/0271678x17740501.
Lavenex, P., Amaral, D.G., 2000. Hippocampal-neocortical interaction: a hierarchy of associativity. Hippocampus 10, 420–430 10.1002/1098-1063(2000)10:4<420::aid-hipo8>3.0.co;2-5.
Leech, R., Sharp, D.J., 2014. The role of the posterior cingulate cortex in cognition and disease. Brain 137, 12–32. https://doi.org/10.1093/brain/awt162.
Liu, R., Chen, H., Qin, R., Gu, Y., Chen, X., Zou, J., Jiang, Y., Li, W., Bai, F., Zhang, B., Wang, X., Xu, Y., 2019a. The altered reconfiguration pattern of brain modular architecture regulates cognitive function in cerebral small vessel disease. Front. Neurol. 10, 324. https://doi.org/10.3389/fneur.2019.00324.
Liu, R., Wu, W., Ye, Q., Gu, Y., Zou, J., Chen, X., Jiang, Y., Bai, F., Xu, Y., Wang, C., 2019b. Distinctive and pervasive alterations of functional brain networks in cerebral small vessel disease with and without cognitive impairment. Dement Geriatr. Cogn. Disord. 47, 55–67. https://doi.org/10.1159/000496455.
Mohan, A., Roberto, A.J., Mohan, A., Lorenzo, A., Jones, K., Carney, M.J., Liogier-Weyback, L., Hwang, S., Lapidus, K.A., 2016. The significance of the default mode network (DMN) in neurological and neuropsychiatric disorders: a review. Yale J. Biol. Med. 89, 49–57.
Nyberg, L., 2017. Functional brain imaging of episodic memory decline in ageing. J. Intern. Med. 281, 65–74. https://doi.org/10.1111/joim.12533.
Nyberg, L., Persson, J., Habib, R., Tulving, E., McIntosh, A.R., Cabeza, R., Houle, S., 2000. Large scale neurocognitive networks underlying episodic memory. J. Cogn. Neurosci. 12, 163–173. https://doi.org/10.1162/089892900561805.
Obler, L.K., Rykhlevskaia, E., Schnyer, D., Clark-Cotton, M.R., Spiro 3rd, A., Hyun, J., Kim, D.S., Goral, M., Albert, M.L., 2010. Bilateral brain regions associated with naming in older adults. Brain Lang. 113, 113–123. https://doi.org/10.1016/j.bandl.2010.03.001.
Pantoni, L., 2010. Cerebral small vessel disease: from pathogenesis and clinical characteristics to therapeutic challenges. Lancet Neurol. 9, 689–701. https://doi.org/10.1016/s1474-4422(10)70104-6.
Petito, C.K., Olarte, J.P., Roberts, B., Nowak Jr., T.S., Pulsinelli, W.A., 1998. Selective glial vulnerability following transient global ischemia in rat brain. J. Neuropathol. Exp. Neurol. 57, 231–238. https://doi.org/10.1097/00005072-199803000-00004.
Promjunyakul, N., Lahna, D., Kaye, J.A., Dodge, H.H., Erten-Lyons, D., Rooney, W.D., Silbert, L.C., 2015. Characterizing the white matter hyperintensity penumbra with cerebral blood flow measures. Neuroimage Clin. 8, 224–229. https://doi.org/10.1016/j.nicl.2015.04.012.
Sam, K., Crawley, A.P., Conklin, J., Poublanc, J., Sobczyk, O., Mandell, D.M., Venkatraghavan, L., Duffin, J., Fisher, J.A., Black, S.E., Mikulis, D.J., 2016. Development of white matter hyperintensity is preceded by reduced cerebrovascular reactivity. Ann. Neurol. 80, 277–285. https://doi.org/10.1002/ana.24712.
Shi, Y., Thrippleton, M.J., Makin, S.D., Marshall, I., Geerlings, M.I., de Craen, A.J., van Buchem, M.A., Wardlaw, J.M., 2016. Cerebral blood flow in small vessel disease: a systematic review and meta-analysis. J. Cereb. Blood Flow Metab. 36, 1653–1667. https://doi.org/10.1177/0271678x16662891.
Tully, P.J., Debette, S., Tzourio, C., 2017. The association between systolic blood pressure variability with depression, cognitive decline and white matter hyperintensities: the 3C dijon mri study. Psychol. Med. 1–13. https://doi.org/10.1017/s0033291717002756.
van Dalen, J.W., Mutsaerts, H.J.M.M., Nederveen, A.J., Vrenken, H., Steenwijk, M.D., Caan, M.W.A., Majoie, C.B.L.M., van Gool, W.A., Richard, E., 2016. White matter hyperintensity volume and cerebral perfusion in older individuals with hypertension using arterial spin-labeling. Am. J. Neuroradiol. 37, 1824–1830. https://doi.org/10.3174/ajnr.A4828.
Wahlund, L.O., Barkhof, F., Fazekas, F., Bronge, L., Augustin, M., Sjogren, M., Wallin, A., Ader, H., Leys, D., Pantoni, L., Pasquier, F., Erkinjuntti, T., Scheltens, P., 2001. A new rating scale for age-related white matter changes applicable to MRI and CT. Stroke 32, 1318–1322. https://doi.org/10.1161/01.str.32.6.1318.
Wierenga, C.E., Benjamin, M., Gopinath, K., Perlstein, W.M., Leonard, C.M., Rothi, L.J., Conway, T., Cato, M.A., Briggs, R., Crosson, B., 2008. Age-related changes in word retrieval: role of bilateral frontal and subcortical networks. Neurobiol. Aging 29, 436–451. https://doi.org/10.1016/j.neurobiolaging.2006.10.024.
Wong, B.Y.X., Yong, T.T., Lim, L., Tan, J.Y., Ng, A.S.L., Ting, S.K.S., Hameed, S., Ng, K.P., Zhou, J.H., Kandiah, N., 2019. Medial temporal atrophy in amyloid-negative amnestic type dementia is associated with high cerebral white matter hyperintensity. J. Alzheimers Dis. 70, 99–106. https://doi.org/10.3233/jad-181261.
Yan, C.G., Wang, X.D., Zuo, X.N., Zang, Y.F., 2016. DPABI: data processing & analysis for (Resting-State) brain imaging. Neuroinformatics 14, 339–351. https://doi.org/10.1007/s12021-016-9299-4.
Ye, Q., Su, F., Shu, H., Gong, L., Xie, C., Zhang, Z., Bai, F., 2017a. The apolipoprotein e gene affects the three-year trajectories of compensatory neural processes in the left-lateralized hippocampal network. Brain Imaging Behav. 11, 1446–1458. https://doi.org/10.1007/s11682-016-9623-5.
Ye, Q., Su, F., Shu, H., Gong, L., Xie, C.M., Zhou, H., Zhang, Z.J., Bai, F., 2017b. Shared effects of the clusterin gene on the default mode network among individuals at risk for Alzheimer's disease. CNS Neurosci. Ther. 23, 395–404. https://doi.org/10.1111/cns.12682.
Zhang, C.E., Wong, S.M., Uiterwijk, R., Backes, W.H., Jansen, J.F.A., Jeukens, C., van Oostenbrugge, R.J., Staals, J., 2019. Blood-brain barrier leakage in relation to white matter hyperintensity volume and cognition in small vessel disease and normal aging. Brain Imaging Behav. 13, 389–395. https://doi.org/10.1007/s11682-018-9855-7.